Article

Pilot-Scale Ultrafiltration of an Emulsified Oil Wastewater

J. Marchese, N. A. Ochoa, C. Pagliero, and C. Almandoz

More About This Article

Additional resources and features associated with this article are available within the HTML version:

- Supporting Information
- Links to the 1 articles that cite this article, as of the time of this article download
- Access to high resolution figures
- Links to articles and content related to this article
- Copyright permission to reproduce figures and/or text from this article

View the Full Text HTML

Pilot-Scale Ultrafiltration of an Emulsified Oil Wastewater

J. M A R C H E S E,*,†,‡ N. A. O C H O A,‡
C. P A G L I E R O,§ A N D C. A L M A N D O Z†,‡

Centro Regional de Estudios Avanzados y Tecnológicos (CREACyT), Gob. de San Luis, Argentina, Laboratorio de Ciencias de Superficies y Medios Porosos, UNSL-CONICET-FONCYT, C.C. 256-5700 San Luis, Argentina, and Facultad de Ingeniería, UNRC-CONICET, Chacabuco y Pedernera, C.C. 256-5700 San Luis, Argentina

Wastewater from a household appliance factory containing emulsified oil was treated using a separation method based on an ultrafiltration membrane. Initial wastewater characteristics were a chemical oxygen demand (COD) of 1500 mg of O_2/L and a total hydrocarbon concentration (HC) of 170 mg/L. The cross-flow pilot-scale study was performed with two commercial spiral-wound membrane modules having a molecular weight cutoff of 35 000 (M2 membrane) and of 2000 (M1 membrane). The M1 membrane showed COD and HC rejection performance higher than the M2 membrane. The M1 permeate flux and solute rejection were investigated in relation to the membrane pressure drop ($\Delta P = 100-400$ kPa), temperature (20−35 °C), and feed cross-flow rate (2−5 m³/h). The permeate flux was in good agreement with the expression of Darcy's law, where the end-of-permeate flux is directly proportional to both applied pressure and temperature. Results indicate that the fouling layer resistance of the membrane was the dominant resistance and that it was mainly caused by the emulsified oil adsorption on the surface and/or in the pore wall of the membrane. For design purposes, correlations to estimate both permeate flux and COD-HC concentration in the retentate or permeate at any operational conditions (temperature, pressure, solution viscosity, concentration factor) have been obtained. Experimental pilot-scale tests had shown that an M1 ultrafiltration membrane is effective for removing emulsified oil and achieving up to 90.1% and 99.7% removal of COD and HC, respectively, with a permeate flux of 20 L h⁻¹ m⁻² at $\Delta P = 400$ kPa and 35 °C. It is pointed out that by optimizing the process design utilizing this membrane module, it is possible to successfully apply the ultrafiltration membrane technology to the treatment of industrial emulsified oil waste effluents.

Introduction

Large amounts of oily wastewaters are generated daily by a variety of industrial sources. An important fraction of these are oil/water emulsions for which current treatment technologies are often costly and ineffective. In a typical oily wastewater plant, the various unit operations may include skimming, emulsion breaking, dissolved air flotation, gravity separation, chemical demulsification, etc. Additional unit operations may be used to improve the effluent quality as dictated by the nature of the wastewater and the effluent standards. In recent years, membrane processes such as microfiltration (MF), ultrafiltration (UF), nanofiltration (NF), and reverse osmosis (RO) are increasingly being applied for treating oily wastewater (*1*, *2*). MF/UF have been successfully used in oil-in-water separation. This is a pressure-driven membrane technique that uses porous membranes for the separation of material in the 1 nm−50 μm size range or compounds with molecular masses in excess of 5000 Da.

Of the three broad categories of oily wastes (free-floating oil, unstable oil/water emulsions, and highly stable oil/water emulsions) membranes are more useful with stable oil/water emulsions, particularly water-soluble oily wastes (*1*). Several researchers have reported on the effectiveness of MF/UF in treating oily wastewaters. Cheryan and Rajagopalan (*3*) described several case studies of membrane applications in a hybrid system when combined with conventional chemical treatment systems to concentrate sludges and discussed the possible pitfalls as well as the potential of applying membranes to the treatment of oily wastes. Bodzek and Konieczny (*4*) reported oil reduction of 95−99% and chemical oxygen demand (COD) reductions of 91−98% in the UF permeate from a metal industry emulsion. Reed et al. (*5*) reported pilot-scale results of the treatment of an oil/grease (O/G) wastewater using UF, with O/G removed efficiencies (rejections) averaging 97−98% and total suspended solids rejections of approximately 97%. Duong et al. (*6*) quantified membrane performance for the UF of a heavy oil. Membrane performance was evaluated in terms of both flux and separation, using ceramic membranes of various pore sizes, and operated over a range of cross-flow velocities and temperatures.

The removal of water from oil-in-water emulsion by a UF membrane was investigated by Hu and co-workers (*7*) in both laboratory- and pilot-scale studies. The effects of membrane material, molecular weight cutoff (MWCO), operating conditions, and oil concentration in emulsion on UF behavior were studied. They found that, for polyacrylonitrile and poly(vinylidene fluoride) membranes, the permeate fluxes are higher than that of polyether sulfone membrane. Experimental results showed that membranes with either high or low MWCO had high separation efficiencies.

Cross-flow MF/UF are of particular interest in processes that demand continuous or semi-continuous operation. However, use in wastewater treatment applications has remained limited as a result of permeate fluxes due to membrane fouling (*8*−*10*). Several approaches to solve this problem have been attempted, among them back pulsing (*11*), vibratory or centrifugal devices to enhance shear at the membrane surface to decrease concentration polarization, modification of membrane surfaces to increase hydrophilicity, and pretreatment of feed (*1*, *12*).

Anderson and Saw (*13*) examined the feasibility of designing a membrane surface that would enhance the separation of oil from oil/water suspensions using cross-flow filtration. The surface characteristics of both UF and MF membranes were modified by adsorption with a non-anionic surfactant composed of polyethylated linear aliphatic alcohols, resulting in a significant improvement in oil rejection.

The most successful UF separation performance is obtained when discrete and stable emulsion particles of oil

---

* Corresponding author fax: 42-2652-430224; e-mail: marchese@unsl.edu.ar.
† CREACyT.
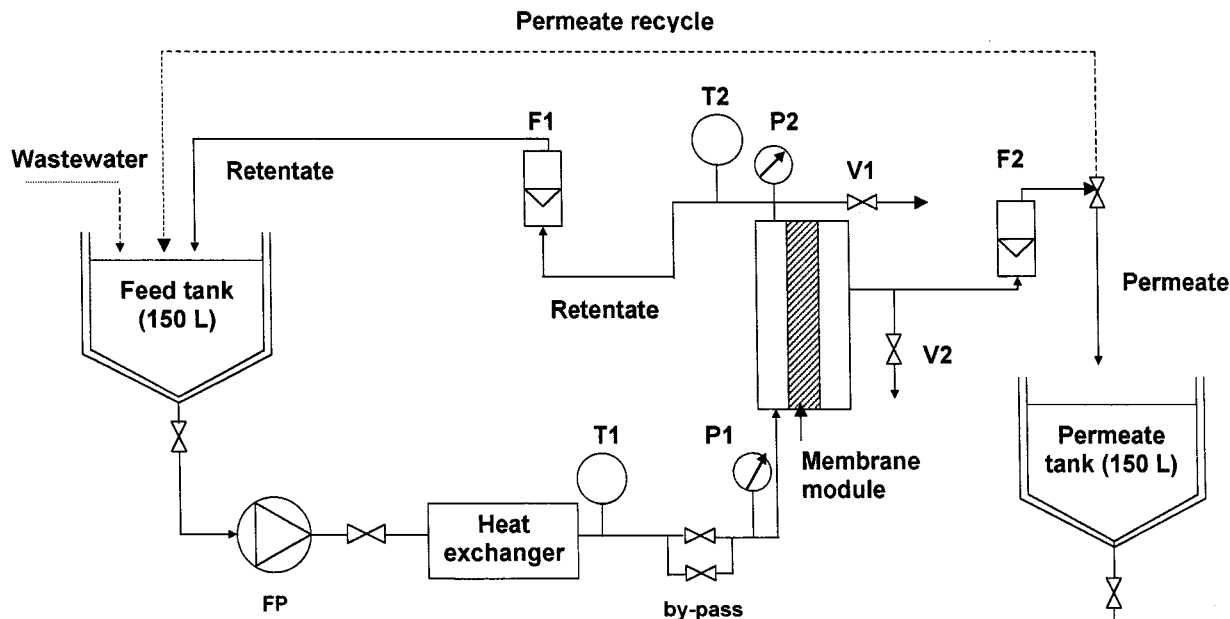‡ UNSL-CONICET-FONCYT.
§ UNRC-CONICET.

FIGURE 1. Scheme of ultrafiltration pilot plant: FP, feed pump; F1 and F2, retentate and permeate flowmeters; T1 and T2, retentate inlet and outlet temperature gauge; P1 and P2, retentate inlet and outlet pressure gauges; V1 and V2, retentate and permeate sample valves.

that are larger than the membrane pore size are maintained. However, the basis for selecting membrane material and membrane operating conditions to achieve adequate rejections of emulsified oil and COD in the permeate water while permeate flux is maintained remains largely empirical. This includes MWCO, pore size distribution, transmembrane pressure, temperature, physicochemical characteristics of the feed solutions, cleaning of the membrane, and other criteria.

This paper reports the results of an experimental pilot-scale study of emulsified oil wastewater ultrafiltration using commercial polymeric membranes. Experiments were performed with wastewater from a local household appliance factory containing emulsified oil. Such wastes cannot be discharged untreated into municipal wastewater treatment plants or rivers. The usual treatment method is flocculation and precipitation by chemicals.

Experimental Section

Apparatus. A schematic diagram of the batch pilot-scale ultrafiltration unit operated in this study is shown in Figure 1. The unit included a spiral-wound ultrafiltration membrane placed in a stainless steel housing, feed and permeate tanks, feed sanitary centrifugal pump, recycle and permeate flowmeters, and heat exchanger. The feed pump had a closed impeller with six reversed blades especially fit to transfer liquid at media-high pressure to optimize the hydraulic efficiency. The feed pump had a maximum discharge pressure of 6×10^5 Pa and a maximum capacity of 6 m^3 h^{-1}. An Alfa-Laval's P-30 plate-type heat exchanger is included in the feed stream to control temperature. Pressure and temperature measurements were obtained from thermocouples and pressure transducers located at the membrane inlet and outlet. Two 150-L stainless steel tanks were used as reservoirs of the feed suspension and permeate solution. The recycle retentate and permeate flows were measured with variable section flowmeters (Gemu 800/850).

Procedure. In this study, the pilot-scale unit was operated in two variations of the batch mode operation. In the first batch mode (batch I), the retentate is fully returned to the feed tank for recycling through the module. The contaminant concentration in the feed tank increases steadily with operation time. Because of the operational capability of the

pilot plant unit, a volume concentration ratio (VCR) or concentration factor (CF) of 3 was fixed as the end of the batch I experimental runs. In the second batch mode of operation (batch II), the startup is the same as the first batch mode system in that the retentate is initially recycled. When the final required concentration factor is reached within the loop, permeate and retentate are totally recycled to the feed tank over a period of 60 h, keeping constant both the concentration and the volume in the feed tank. The batch I operation was used to determine rejection coefficients from permeate data and volume concentration ratio. Batch II was used to analyze the effect of long-term experiments on membrane performance.

Tests were carried out at different temperatures and transmembrane pressures. The experimental conditions were as follows: feed flow rate between 2 and 5 m^3 h^{-1}, transmembrane pressure of 100−400 kPa, and feed temperature of 20−35 °C.

The experimental selection criteria were established to facilitate performance of the pilot study in a number of different ways. The transmembrane pressure and temperature operation criterion was set to reduce the risk of membrane integrity problems or irreversible fouling.

Membranes. The pilot-scale unit operated with two industrial spiral-wound membrane modules, denoted as M1 (MOCU4040U20) and M2 (MOPS4040U006) provided by SEPAREM S.P.A. (Italy). The M1 and M2 membranes had a MWCO of 2000 and 35 000, respectively. The thin-film composite M1 membrane was constructed of polyamide deposited onto a polysulfone support. The asymmetric M2 membrane was made of polysulfone material. Both membranes had a transfer area of 9 m^2, and their characteristics are given in Table 1.

Membranes were reused after each experiment, following an elaborate physical and chemical cleaning procedure. After each experiment, the emulsified oil/water solution was removed from the feed tank and pipelines. Then fresh tap water was placed into the feed tank and circulated through the membrane. The membrane was physically cleaned for a total of 30 min with the retentate and permeate being recycled into the feed tank. At the conclusion of physical washing, an 8×10^{-3} M HNO$_3$ solution was prepared in the feed tank and recycled through the membrane for 1 h. At the

TABLE 1. Characteristics of Industrial Spiral-Wound Modulus

characteristics parameters	module type	
	M1	M2
configuration	spiral wound	spiral wound
dimension		
length (m)	1.0	1.0
external diameter (m)	0.1	0.1
flat sheet width (m)	9	9
channel (spacer) height (m)	0.75×10^{-3}	1×10^{-3}
membrane material	polyamide	polysulfone
membrane area (m^2)	9	9
max pressure inlet (bar)	42	10
typical operational pressure (bar)	3–28	2–10
max operational temp (°C)	50	50
pH range	2–11	2–11
hydraulic permeability at 30 °C ($L\,m^{-2}\,h^{-1}\,kPa^{-1}$)	7.92×10^{-2}	28.80×10^{-2}
MWCO (Da)	2000	35000

TABLE 2. Physicochemical Characteristics of the Effluent

appearance	turbid
pH	9.5
COD (mg of O_2/L)	1500
hydrocarbons (HC) (ppm)	170
turbidity (g/L of $BaSO_4$)	0.45
density at 20 °C (g/cm^3)	1.006
Cr(VI) (ppb)	30.1
Cd (ppb)	0.18
Pb (ppb)	24.6
As (ppb)	0.148
emulsion–oil suspensions (μm)	<0.2

end of the chemical cleaning, the detergent solution was removed from the apparatus. Tap water was fed into the feed tank, and the residual detergent of the membrane was purged into the tank. Finally, distillate water was circulated through the membrane for 2 h, and permeate flux was determined. The chemical cleaning procedure was repeated until the permeate flux of the cleaned membrane was similar to that of the virgin membrane (97–99%).

Effluent. A local household appliance factory supplied the wastewater effluent sample. Wastewater contained emulsified oil, primarily from tap water and deionized water that were used to wash and rinse the sheets of metal. The sheet surface was covered with a thin film of mineral oil comprising 10.6% aromatics and an aniline point of 59.5 °C. The oil was removed from the sheet with a nonionic detergent (oxyethylene nonyl phenol). There is about 45 m^3 of such wastewater produced in this factory every day. The main physicochemical characteristics of the effluent are given in Table 2. Because of the high COD of up to 1500 mg/L and the total hydrocarbons (HC) of 170 mg/L, such wastes cannot be discharged untreated.

Analytical Methods. *Determination of HC.* Dissolved or emulsified oil was extracted from water by intimate contact with an extracting solvent. The gain in weight of the tared distilling flask was the amount of oil in the sample [5520A, Standard Method for the Examination of Water and Wastewater (SMEWW)].

COD. A sample was refluxed in strongly acid solution with a known excess of potassium dichromate. Oxygen consumed was measured against standards at 600 nm by UV–visible UNICAM spectrophotometer (5220B SMEWW).

BOD. BOD was evaluated following the 5210B SMEWW.

Metals were determined by atomic absorption spectrometry, and solution viscosities were determined using an Ubbelohde viscometer.

Theoretical Fundamentals: Design Parameters

Physical Aspects of UF Process. The permeate flux, J, is an important parameter in the design and analysis of the economic feasibility of the UF separation process. Hydrodynamics of membrane modules have an important effect on the mass transfer, separation, and fouling behavior of membrane systems.

Generally, the pure solvent transport through porous UF membranes is directly proportional to the applied transmembrane pressure (ΔP). Models that can be used to describe the convective flow (J_0) are the Kozeny–Carman and Hagen–Poiseuille equations:

$$J_0 = \frac{\Delta P}{\eta_o R_m} \qquad (1)$$

where η_o is the solvent viscosity and R_m is the intrinsic resistance of the clean membrane.

When solutes are present, there is a permeate flux decline due to membrane fouling (*14*). A decrease in flux is a rather complex phenomenon involving adsorption of macromolecules to the membrane surface and involving pore blocking, concentration polarization, and formation of a gel-like cake layer within membrane pores (*15*). Several models have been used to describe solute fouling, among them hydraulic resistance, osmotic pressure, gel polarization, and film models (*16–19*).

Darcy's law (also known as the resistance-in-series theory) is widely used to relate the permeate flux (J) to the applied pressure and the fouling resistance (*20*):

$$J = \frac{\Delta P}{\eta (R'_m + R_p)} \qquad (2)$$

Here, η is the solution viscosity, and R'_m ($= R_m + R_f$) is the intrinsic membrane resistance that includes the fouling layer resistance (R_f) due to specific membrane–solute interactions. R_p is the polarization layer resistance, which consists of two resistances: R_g due to the gel-polarized layer and R_b due to the associate boundary layer. The intrinsic membrane resistance is unaffected by operating parameters whereas the polarization layer resistance is a function of applied pressure. When R_p is negligible, the filtrate flux is given by

$$J = \frac{\Delta P}{\eta R'_m} = \frac{\Delta P}{\eta (R_m + R_f)} \qquad (3)$$

Design Parameter. To quantitatively estimate the relative degree of purification in a given UF process or to evaluate the period of UF processing required to attain a certain degree of separation or purification, the UF process must be mathematically modeled (*1*). The observed rejection coefficient at any point in the UF process is defined as $R = 1 - (C_p/C_r)$ where C_p and C_r are the bulk solute concentration in the permeate and retentate, respectively.

During UF membrane operation, there is a volume rejection because contaminants are not degraded or destroyed. Thus, ultrafiltration data can be presented in terms of volume concentration ratio (VCR) or concentration factor (CF):

$$\text{VCR} = \text{CF} = \frac{V_0}{V_r} = 1 + \frac{V_p}{V_r} \qquad (4)$$

where V_0 is the initial feed tank volume and V_r and V_p are the retentate and permeate volumes, respectively.
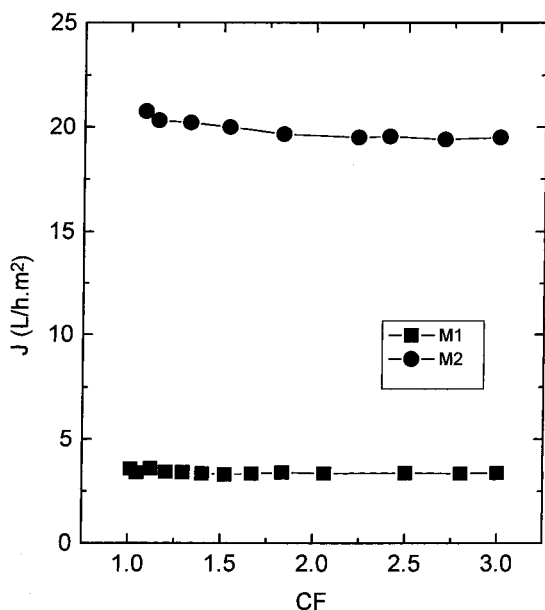
FIGURE 2. Permeate flux as a function of concentration factor of M1 and M2 membranes, operated at T = 20 °C, ΔP = 200 kPa, and F_v = 3 m³/h.

The material balance at any time during UF operation is given by

$$\log(\text{SCR}) = \log\left(\frac{C_r}{C_0}\right) = R\log(\text{CF}) \tag{5}$$

where SCR is the solute concentration ratio and C_0 is the initial solute concentration in the feed. Equation 5 shows that the solute retentate concentration at any time or stage of UF processing is a function of both the concentration factor and the rejection coefficient. This equation allows the calculation of rejection using only retentate data (C_r, V_r).

Results and Discussion

Membrane Selection. It is well-known that ultrafiltration may be able to retain macromolecules such as colloids, proteins, etc. This process has the advantage of a relatively high permeate flux and a low/medium transmembrane pressure drop. The high selectivity and flux results in high efficiency and short processing time.

When the cutoff or pore size of the membrane is decreased, its rejection capacity increases, but higher transmembrane pressure is needed to reach an acceptable permeate flux rate. At first, the effect of decreasing membrane pore size on membrane performance with raw wastewater was tested. Experiments were conducted at a temperature of 20 °C, feed flow of F_v = 3 m³/h, and membrane pressure of 100 kPa. The system was operated in batch I mode. Permeate flux and solute concentration ratio for both COD and HC as a function of concentration factor are summarized in Figures 2 and 3, respectively. The linear regression between log(SCR) and log(CF) was carried out according to eq 5 to evaluate the R values from the slopes given in Figure 3.

In general a decrease in the membrane cutoff (pore size) resulted in an increase in the degree COD and HC retention and a decrease in the permeate flux. The average end-of-permeate flux decreased from 20 to 3.4 L m^{-2} h^{-1} when the membrane cutoff decreased from 35 000 to 2000 Da, whereas the COD and HC rejections increased respectively from 18 to 89% and from 25 to 99%. These results show that M1 membrane COD and HC rejection performance were significantly higher than in the M2 membrane. The M1
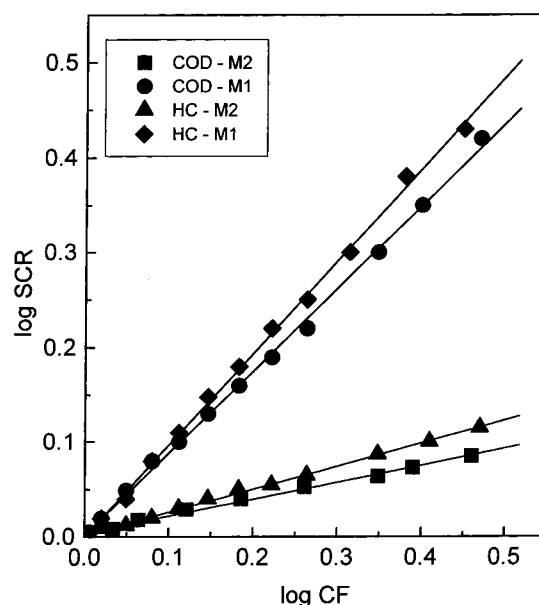

FIGURE 3. Solute concentration ratio as a function of concentration factor of M1 and M2 membranes operated at T = 20 °C, ΔP = 200 kPa, and F_v = 3 m³/h.

membrane was chosen for further study because of its higher COD–HC retention.

Effect of Feed Cross-Flow Velocity. It is well-known that increasing cross-flow velocity increases both the mass transfer coefficient across the concentration polarization boundary layer and the degree of mixing near the membrane surface, thereby reducing both the accumulation of a gel layer on the membrane surface, and the fouled membrane resistance (*1*, *2*). Hence the effect of feed cross-flow velocity on M1 membrane performance was investigated. The spiral-wound modules are basically flat sheets separated by a mesh-like spacer to form a narrow slit for fluid flow. The cross-sectional area is $a \times b$, where a is the width of the flat sheet and b is the channel (spacer) height. For feed flow between 2 and 5 m³/h and the $a-b$ values given in Table 1, the liquid velocity through the channel of M1 membrane should range from 290 to 730 m/h, corresponding to Reynolds numbers of 122–307 (laminar flow region). However, the additional turbulence contributed by the spacers should be taken into account. The state of turbulence can be determined by the following general relationship (*22*):

$$\Delta P = f(F_v)^n \tag{6}$$

with n = 1 for laminar flow and n = 1.5–1.9 for turbulent flow. To determine the state of turbulence for M1 membrane, a series of experiments with pure water was carried out at feed cross-flow between 2 and 5 m³/h (T = 35 °C). Data were well fitted by the following correlation:

$$\Delta P = 0.029 F_v^{1.95} \tag{7}$$

The n value of 1.95 indicates that the system is working in the turbulent flow regimen.

Operating in the batch I mode at T = 35 °C and ΔP = 400 kPa, the effect of different cross-flow velocities between 2 and 5 m³/h with emulsified oil solution was examined. The data of Figure 4 show that for a feed flow rate higher than 2 m³/h, the end-of-permeate flux (J) was not a strong function of cross-flow velocity, corroborating that a high turbulent flow is produced in the range of operating conditions considered here.
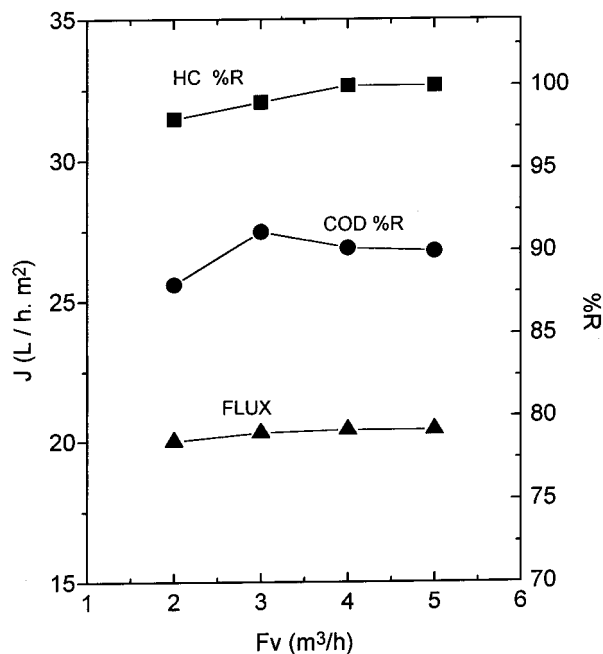
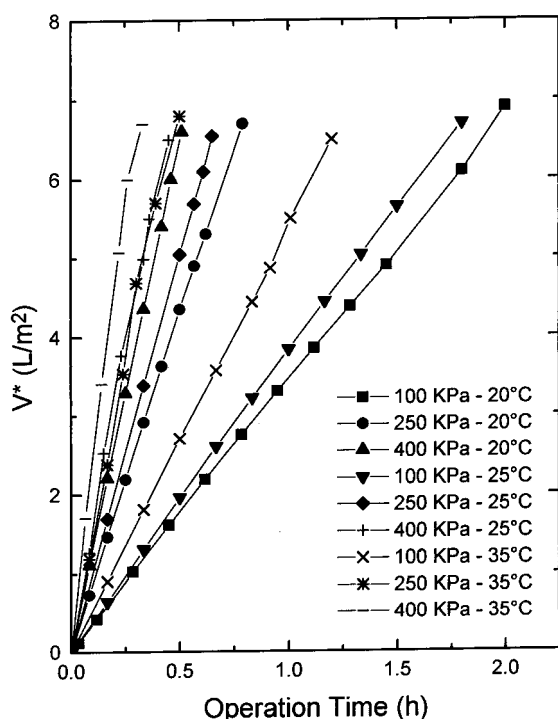FIGURE 4. Effect of feed cross-flow velocity on end-of-permeate flux and COD-HC rejections for M1 membrane operated at T = 35 °C and ΔP = 400 kPa.

FIGURE 5. Permeate volume per membrane area as a function of operation time and membrane pressure drop (T = 20, 25, and 35 °C; F_v = 3 m³/h).

Effect of Temperature and Pressure on M1 Performance.

According to Darcy's law, flux can be increased by reducing viscosity or increasing transmembrane pressure, although fouling effects may limit the increase that can be achieved (21). To investigate these effects on M1 performance, a series of experiments in batch I mode were performed at temperatures of 20, 25, and 35 °C; transmembrane pressures of 100, 250, and 400 kPa; and feed cross-flow velocities of 3 m³/h.

Figure 5 shows the results from UF experiments in terms of permeate volume per membrane area (V^*) conducted at
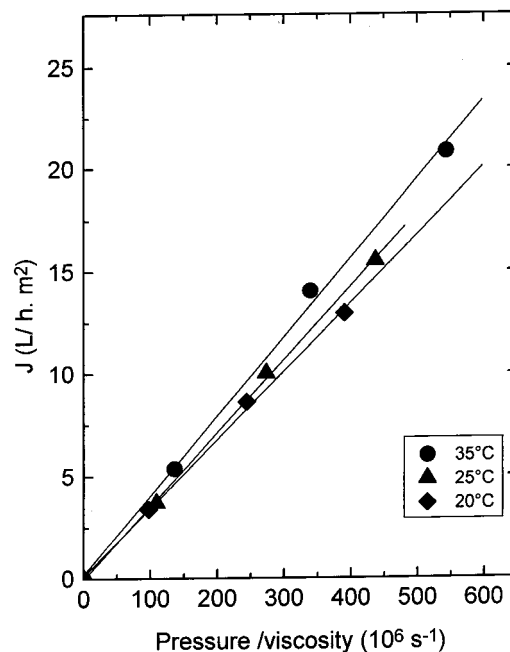

FIGURE 6. End-of-permeate flux versus transmembrane pressure/viscosity ratio at different temperatures.

20, 25, and 35 °C. The linear increase of V^* with operation time points out that end-of-permeate flux remained nearly constant with volumetric concentration factor. Values for J from linear regression between V^* and operation time are given in Table 3, showing that the rate of permeate production is significantly greater at both higher temperature and transmembrane pressure conditions.

Figure 6 shows the linear pressure/viscosity dependence of the end-of-permeate flux. Both the independence of J with cross-flow velocity (Figure 4) and its relationship with $\Delta P/\eta$ (Figure 6) indicate that under these operational conditions the gel-polarization effects are minimal. This is in agreement with eq 3 where flux is directly proportional to the applied pressure and inversely proportional to the viscosity. The intrinsic fouling resistances of the membrane (R'_m) at different temperatures were calculated from the slopes of Figure 6, and their values are listed in Table 3. The intrinsic resistance of the clean membrane ($R_m = 5.676 \times 10^{11}$ m^{-1}), calculated from hydraulic permeability (Table 1), was found to be 2 orders of magnitude smaller than those of the fouling layer resistance ($R_f = 9.26-10.75 \times 10^{13}$ m^{-1}), indicating that R_f was the dominant resistance. From these results, the following general relationship to predict the permeate flux as a function of $\Delta P/\eta$ (s) and T (°C) has been obtained:

$$J\left(\frac{m}{s}\right) = 23.91\, T^{-0.2662}\frac{\Delta P}{\eta} \qquad (8)$$

Additional experiments were carried out in which the clean membrane was wetted for 10 min by the feed solution without applying pressure. A marked decrease in the hydraulic permeability of the membrane after being rinsed by the physical procedure indicates a strong likelihood of prompt fouling. Prompt fouling is an adsorption phenomenon, and it is a very common effect in the commercial membrane. The prompt fouling resistance values of the membrane (R''_m), given in Table 3, were 20–35% lower than R'_m resistance. These results suggest that the membrane fouling was mainly caused by emulsified oil adsorption on the surface and/or the pore wall of, and partially obstructing the passages through, the membrane. In addition to lowering the flux of the membrane, this type of fouling raises the retention.

TABLE 3. Summary of End-of-Permeate Flux, Rejections, and Intrinsic Membrane Resistance Results of M1 Membrane

T (°C)	$\bar{\eta}$ (mPa s^{-1})^a	$\Delta P/\eta$ (10^6 s^{-1})	J (L m^{-2} h^{-1})	COD (% R)	HC (% R)	R'_m (10^{13} m^{-1})	R''_m (10^{13} m^{-1})
20	1.024	97.60	3.39	89	99		
		244.02	8.64	90	98.4	9.32	7.21
		390.43	12.94	91.5	99.3		
25	0.9149	109.30	3.76	87.3	99.1		
		273.26	9.98	90.6	98.7	10.08	7.47
		437.21	14.96	91.1	99.5		
35	0.7365	135.78	5.3	87.45	98.2		
		339.46	14.05	91.4	99	10.81	7.02
		543.13	20.3	91.2	99.7		

^{a} Average viscosity values of the retentate solutions between CF = 1 and CF = 3.

TABLE 4. Summary of Retentate and Permeate Quality (T = 35 °C, ΔP = 400 kPa, and CF = 3)

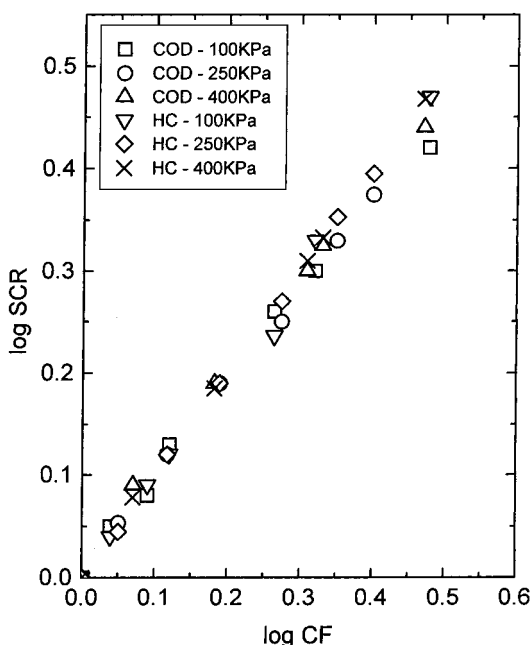| physicochemical parameters	original wastewater (1 stage)		permeate of original wastewater (2 stage)		discharge water regulations
	retentate	permeate	retentate	permeate	
pH	9.5	9.5	9.5	9.5	6−8
COD (ppm)	4029	354	950	83	<100
HC (ppm)	508	1.5	4.5	0.01	<100
Cr(VI) (ppb)	30.1	30.1	30.1	30.1	≤50
Cd (ppb)	0.18	0.18	0.18	0.18	≤1
Pb (ppb)	24.6	24.6	24.6	24.6	≤50
As (ppb)	0.148	0.148	0.148	0.148	≤50
BOD (ppm)	960	94.2	254	24.1	<100

FIGURE 7. Solute concentration ratio as a function of concentration factor of M1 membrane operated at T = 35 °C (ΔP = 100, 250, and 400 kPa).

The data of solute concentration ratio for both COD and HC as a function of concentration factor at 35 °C and different transmembrane pressures are reported in Figure 7. Results from other experimental runs (T = 20 and 25 °C) were similar to those in Figure 7. COD and HC rejections were obtained by least-squares analysis of log(SCR) versus log(CF) slopes according to eq 5. In Table 3, a summary of the permeate flux and COD−HC rejection results is presented. For the range of conditions of the present study, the data in Table 3 suggest that the dominant mechanism of COD−HC rejections was size exclusion of the membrane pores. These results indicate that the M1 ultrafiltration membrane was effective in rejecting the pollutants of emulsified oil wastewater, achieving up to

91.2% and 99.7% rejection of COD and HC, respectively, with permeate fluxes of 3−20 L m^{-2} h^{-1} depending on T and ΔP operation conditions.

From the good linearity between log(SCR) and log(CF) and the insignificant change in COD−HC retention observed over the wide range of operational conditions, the following general correlations have been derived:

$$\text{SCR}_{(\text{COD})} = (\text{CF})^{0.90} \tag{9}$$

$$\text{SCR}_{(\text{HC})} = (\text{CF})^{0.99} \tag{10}$$

These expressions allow the calculation of the COD−HC concentrations in the retentate and permeate at any CF. For design purposes eqs 8−10 together with the solute mass balance are the main correlations to be used.

Long-Term Experiments. The batch II mode experiment was conducted at 400 kPa and 35 °C over a period of 60 h. When the CF of the original wastewater reached 3, both the retentate and the permeate were totally recycled to the feed tank. Quite stable flux and rejections were achieved throughout the experimental period. The average permeate flux of 19.7 ± 1 L m^{-2} h^{-1} and average retention of 91% and 99% for COD and HC, respectively, indicated that the M1 membrane performs rather well and had a reasonably long life at appropriate operating conditions.

Permeate Quality. Table 4 shows how UF one-stage permeate COD (ppm) parameter (35 °C, 400 kPa, CF = 3), which was above those required by the regulations of the Province of San Luis, Argentina, was acceptably low after the one-stage permeate underwent a second identical treatment. The water permeate from the second stage, prior to pH adjustment, has appropriate characteristics for direct discharge into municipal wastewater treatment plants and river ditches, or it can be reused in the wash step of the technological cycle of the household appliances factory.

Literature Cited

(1) Cheryan, M. *Ultrafiltration and Microfiltration Handbook*; Technomic: Lancaster, PA, 1998.

(2) Noble, R.; Stern, S. A. *Membrane Separations Technology. Principles and Appliccations*; Elsevier: Amsterdam, 1995.

(3) Cheryan, M.; Rajagolapan, N. *J. Membr. Sci.* **1998**, *151*, 13−28.

(4) Bozdek, M.; Konieczny, K. *Waste Manage.* **1992**, *12*, 75.

(5) Reed, B. E.; Lin, W.; Dunn, C.; Carriere, P.; Roark, G. *Sep. Sci. Technol.* **1997**, *32* (9), 1493−1511.

(6) Duong, A.; Chattapadhyaya, G.; Kwork, W. Y.; Smith, K. J. *Fuel* **1997**, *76* (9), 821−828.

(7) Hu, X.; Bekassy-Molnar, E.; Vatai, G.; Olah, J. *Chem. Technik* **1998**, *50* (3), 119−123.

(8) Freeman, S. D. N.; Morin, O. J. *Desalination* **1995**, *103*, 19.

(9) Zhu, X.; Elimelech, M. *Environ. Sci. Technol.* **1997**, *31*, 3654−3662.

(10) Song, L.; Hohnaoin, P. R.; Elimelech, M. *Environ. Sci. Techonl.* **1994**, *28*, 1164−1171.

(11) Ramirez, J. A.; Davis, R. H. *J. Hazard. Mater.* **1998**, *B63*, 179−197.

(12) Belkacem, M.; Matamoros, H.; Cebassud, C.; Aurelle, Y.; Cotteret, J. *J. Membr. Sci.* **1995**, *106*, 195−205.

(13) Anderson, G. K.; Saw, C. B. *Environ. Technol. Lett.* **1987**, *8*, 121−132.

(14) Song, L.; Elimelech, M. *J. Chem. Soc., Faraday Trans.* **1995**, *91*, 3389−3398.

(15) Ko, M. K.; Pellegrino, J. J. *J. Membr. Sci.* **1992**, *74*, 141−157.

(16) Fane, A. G. Ultrafiltration: Factors influencing flux and rejection. In *Progress in Filtration and Separation*; Wakeman, R. J., Ed.; Elsevier: Amsterdame, 1986; pp 101−179.

(17) Hermia, J. *Trans. Inst. Chem. Eng.* **1982**, *60*, 183.

(18) McCabe, W. L.; Smith, J. C.; Harriott, P. *Unit Operation of Chemical Engineering*; McGraw-Hill: New York, 1985.

(19) Prádanos, P.; Hernandez, A.; Calvo, J. I.; Tejerina, F. *J. Membr. Sci.* **1996**, *114*, 115−126.

(20) Belfort, G.; Davis, R. H.; Zydney, A. L. *J. Membr. Sci.* **1994**, *96*, 1−58.

(21) Mulder, M. *Basic Principles of Membrane Technology*; Kluwer: Dordrecht, 1990.

(22) Cheryan, M.; Chiang, B. H. *Food Process Engineering*, Vol. 1; McKenna, Ed.; 1984.